Highlights of Spanish Astrophysics VII, Proceedings of the X Scientific Meeting of the Spanish Astronomical Society held on July 9 - 13, 2012, in Valencia, Spain. J. C. Guirado, L. M. Lara, V. Quilis, and J. Gorgas (eds.)

Probing nuclear activity versus star formation at $z \sim 0.8$ using near-infrared multiobject spectroscopy

C. Ramos Almeida[1,2], J. M. Rodríguez Espinosa[1,2], J. A. Acosta-Pulido[1,2], A. Alonso-Herrero[3,4], A. M. Pérez García[1,2], and N. Rodríguez-Eugenio[1,2]

[1] Instituto de Astrofísica de Canarias, C/Vía Láctea, s/n, E-38205, La Laguna, Tenerife
[2] Departamento de Astrofísica, Universidad de La Laguna, E-38205, La Laguna, Tenerife
[3] Instituto de Física de Cantabria, CSIC-Universidad de Cantabria, E-39005 Santander
[4] Augusto González Linares Senior Research Fellow

Abstract

We present near-infrared (NIR) spectroscopic observations of 28 X-ray and mid-infrared sources at a median redshift of $z \sim 0.8$ in the Extended Groth Strip (EGS). To date this is the largest compilation of NIR spectra of active galactic nuclei (AGN) at this redshift. The data were obtained using the multi-object spectroscopic mode of the Long-slit Intermediate Resolution Infrared Spectrograph (LIRIS) at the 4.2 m William Herschel Telescope (WHT). These AGN are representative of a larger sample studied in a previous work, consisting of over a hundred X-ray selected AGN with mid-infrared counterparts, which were classified either as AGN-dominated or host galaxy-dominated (i.e. buried AGN) depending on the shape of their spectral energy distributions (SEDs). Here we present new NIR spectra of 13 and 15 sources of each class respectively. We detect the Hα line at $\geq 1.5\,\sigma$ above the continuum for the majority of the galaxies. Using attenuation-corrected Hα luminosities, and after subtracting an AGN component that we estimate using an AGN empirical correlation, we obtain a median star formation rate (SFR) of 7 ± 7 M$_\odot$ year^{-1}. This SFR is lower than those reported in the literature for different samples of non-active star-forming galaxies of similar stellar masses and redshifts ($M_* \sim 10^{11}$ M$_\odot$ and $z \sim 1$). Despite the small size of the sample, we speculate on the possibility of AGN quenching the star formation in galaxies at $z \sim 0.8$. Alternatively, we might be seeing a delay between the offset of the star formation and the AGN activity, as observed in the local Universe.

1 Introduction

The star formation activity in the hosts of AGN at $z \sim 1$ has been studied by several authors using mid-infrared (MIR), far-infrared (FIR), and submillimiter data [1, 4, 3, 12, 18]. The latter authors found that the period of moderately luminous AGN activity does not seem to have strong influence in the star formation activity of the galaxies, in contradiction with the results found at low redshift (e.g. [9]).

The work presented here is a summary of [15], and constitutes a spectroscopic follow-up of a representative subset of the sample of X-ray and mid-infrared sources studied in [14]. Here we present NIR spectroscopic observations for 28 of these sources, which have spectroscopic redshifts in the range $z = [0.27, 1.28]$, and a median redshift of $z = 0.76$. Throughout this paper we assume a cosmology with $H_0 = 75$ km s^{-1} Mpc^{-1}, $\Omega_{\rm m} = 0.27$, and $\Omega_\Lambda = 0.73$.

2 Sample and near-infrared spectroscopic data

The AGN sample studied in [14] was originally selected by [2] in the X-rays, using Chandra data from [13] and XMM-Newton data from [21]. At the flux limits of these X-ray surveys, most of the sources are expected to be AGN. [2] considered only the 138 objects with secure detections in the four Spitzer/IRAC bands (3.6, 4.5, 5.8, and 8 μm) and Spizer/MIPS 24 μm band. Of the 138 sources in the [2] sample, we discarded 42 galaxies that showed multiple detections in the ground-based images (optical and NIR) to avoid source confusion in the Spitzer MIR fluxes. See [14] for a detailed description of the data, photometric redshift calculations, and SED classification. The sources were then classified in five main categories in terms of the template used to fit their SEDs: *starburst-dominated*, *starburst-contaminated*, *type-1 AGN*, *type-2 AGN*, *normal galaxy*.

Our main goal in [14] was to classify the galaxies into these five groups and study their properties. It is worth clarifying that all of the sources are, in principle, AGN, on the basis of their X-ray and MIR emission, but only those included in the type-1, type-2 and starburst-contaminated (SB-cont) groups have AGN-dominated SEDs. It is possible, however, that a small percentage of the sample corresponds to star-forming galaxies emitting in the X-rays and MIR (see e.g. [16]). To confirm the dominance/presence of the AGN over the star formation/host galaxy emission and vice-versa, and to estimate SFRs from the Hα emission, we obtained NIR spectroscopic data for a subsample of 28 galaxies ($\sim 30\%$ of the total sample), which are representative of the five groups described above. The NIR spectroscopic observations were done from 2008 March to 2009 May using the multi-object spectroscopic (MOS) mode of the NIR camera/spectrometer LIRIS on the WHT. The spatial scale of the LIRIS detector is 0.25 arcsec pixel^{-1}.

Four masks were designed and the chosen slit-width was 0.85 arcsec, with the lengths varying between 8.5 arcsec and 12 arcsec, allowing enough space for nodding while avoiding overlap of the spectra. We used the low-resolution grism ZJ, which covers the range 0.8–1.4 μm, providing a spectral resolution of ~ 500 km s^{-1} with the 0.85 arcsec slits. We extracted the individual spectra for each galaxy and reference star, using an aperture of

1 arcsec, matching the maximum value of the seeing during the observations. Examples of the observed NIR spectra of the 28 AGN are shown in Fig. 1.

For 20 of the galaxies in the sample observed with LIRIS there are publicly available spectroscopic data from the Deep Extragalactic Evolutionary Probe 2 (DEEP2; [7]). Our main interest in having optical spectra of our galaxies is to measure Hβ fluxes for those galaxies with Hα detected in the NIR, and thus determine individual values of the extinction to correct our Hα fluxes.

3 Results

After scaling the DEEP2 spectra to the flux-calibrated LIRIS data, we measured the fluxes of the emission lines. We fitted Gaussian profiles using the Starlink program DIPSO. For several faint/undetected transitions, the continuum noise was used to calculate a 1.5 σ upper limit to the line emission. By putting together the optical and NIR spectra of the galaxies, we have emission line flux measurements of Hα for 18/28 galaxies and upper limits for another five. We have calculated Hα luminosities ($\mathrm{L_{H\alpha}}$) using the corresponding luminosity distances. In order to obtain SFRs for the galaxies in the sample using their Hα luminosities, we have to correct $\mathrm{L_{H\alpha}}$ from attenuation, using the A_V values that we calculated using the Hα and Hβ narrow-line fluxes, when available, and the standard Galactic extinction curve of [5] with $R_V = 3.1$.

From the comparison between the spectroscopic data, the X-ray luminosities and the SED classification presented in [14], we cannot confirm the presence of nuclear activity in 4/28 sources (14% of the sample), namely G47, G55, G62 and G107. These galaxies: 1) have L_{X} compatible with a star-forming origin, as defined by [16], 2) have SEDs that we fitted with galaxy or starburst templates, and 3) lie outside the AGN region in Figures 11 and 12 in [15]. In the following, we will exclude these four galaxies from the results found for AGN.

The Hα emission in quiescent (i.e. non-active) galaxies is produced almost entirely by massive stars ($M > 10$ $\mathrm{M_\odot}$), but in active galaxies it includes a contribution from gas photoionised by the AGN. In fact, this contribution will dominate in the case of pure AGN, and it will be, in principle, less important in the case of buried AGN. To test the latter, in Fig. 2 we represent $L_{\mathrm{H}\alpha}$ versus $L_{2-10\ \mathrm{keV}}$. If we consider the 2–10 keV luminosity as a proxy of the AGN, it should be correlated with $L_{\mathrm{H}\alpha}$ for AGN-dominated objects. Thus, we can derive an empirical relationship between $L_{\mathrm{H}\alpha}$ and L_{X} using the four galaxies that we can definitely classify as AGN-dominated from their spectra, SED fits, and diagnostic diagrams presented in this work: G60, G63, G78, and G93. By fitting them, we find a correlation in the form $\log(L_{\mathrm{H}\alpha}) = 0.95 \log(L_{\mathrm{X}}) + 0.39$.

We use the AGN empirical correlation to calculate, for a given L_{X}, the expected $L_{\mathrm{H}\alpha}^{\mathrm{AGN}}$ of the galaxies. We then subtract this AGN contribution from the attenuation-corrected $L_{\mathrm{H}\alpha}^{\mathrm{corr}}$ values to obtain $L_{\mathrm{H}\alpha}^{\mathrm{SF}}$ (see Table 1). For the galaxies below the correlation ($L_{\mathrm{H}\alpha} < L_{\mathrm{H}\alpha}^{\mathrm{AGN}}$) and for those without 2–10 keV luminosities, we cannot estimate the AGN contribution to Hα, and thus we have used the total $L_{\mathrm{H}\alpha}$ values as upper limits. We can now estimate reliable SFRs for the galaxies in our sample using our individual $L_{\mathrm{H}\alpha}^{\mathrm{SF}}$ values and the [10] conversion

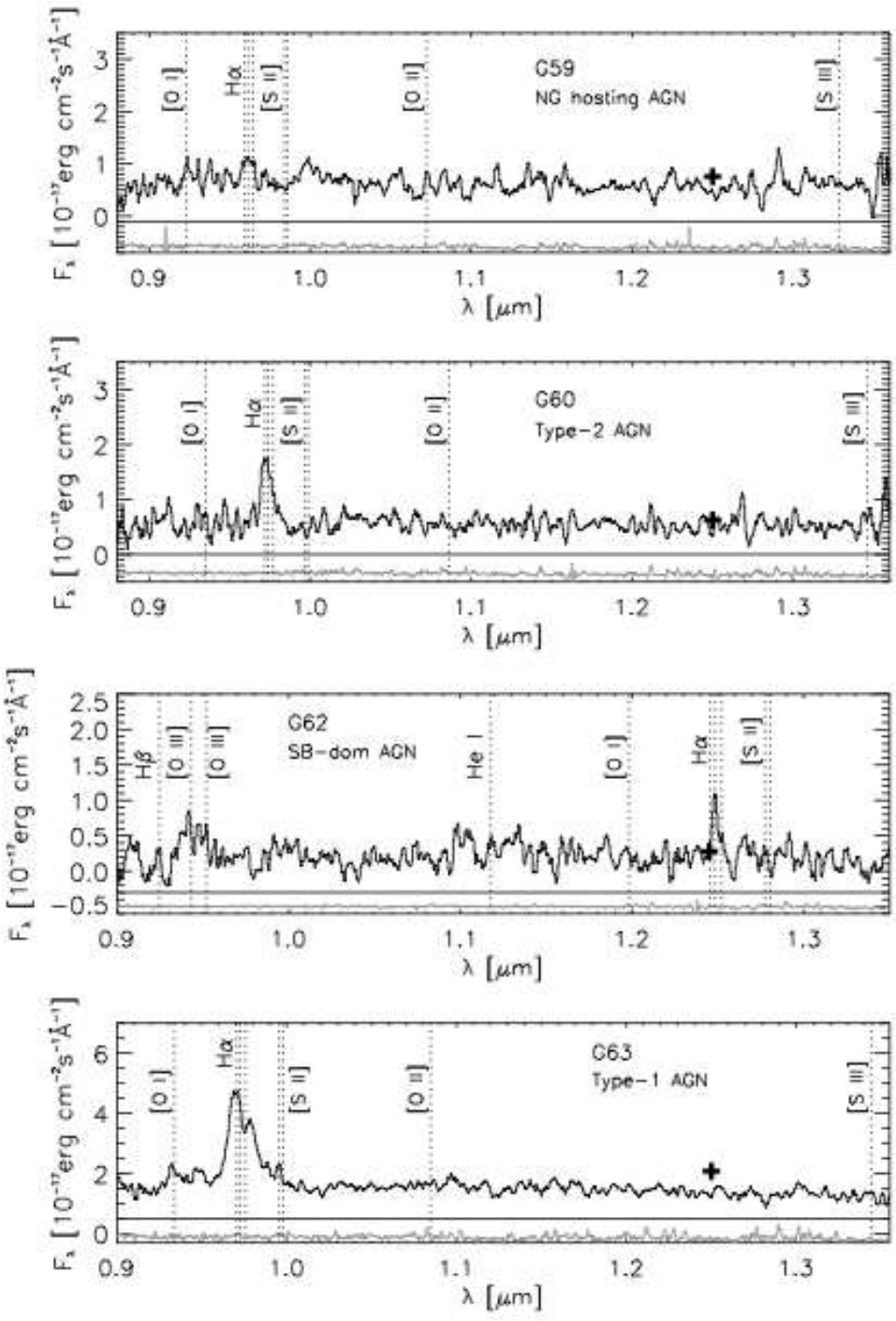

Figure 1: Observed NIR LIRIS spectra of four galaxies. Typical AGN emission lines are labelled. The Hα labels correspond to Hα + 2[NII]. The SED classification from [14] is indicated at the top of each panel, and an scaled sky spectrum for each galaxy is plotted at the bottom. Observed J-band fluxes are represented with a cross for comparison.

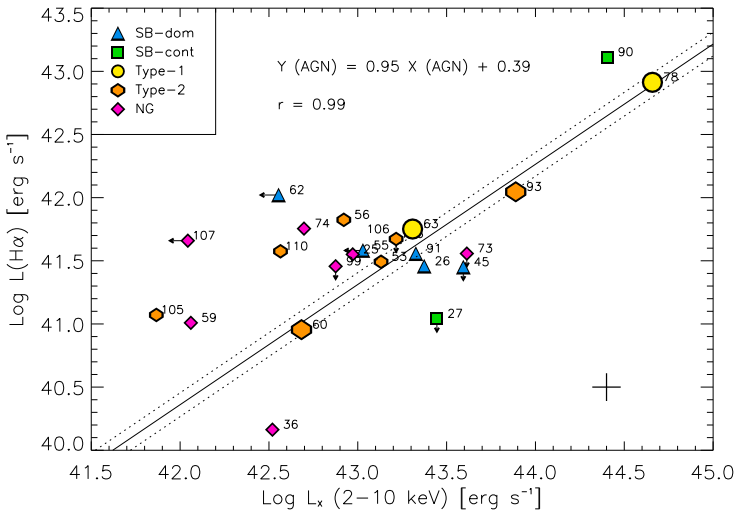

Figure 2: Hα versus hard X-ray luminosity (2–10 keV). Solid line corresponds to the AGN empirical relationship determined using the four AGN-dominated galaxies (plotted with larger symbols). Objects well above this line are likely dominated by star formation, whereas those below may have Hα fluxes affected by extinction.

for Case B recombination at $T_{\rm eff} = 10,000$ K, assuming solar metallicity and a [11] initial mass function (IMF): SFR($M_\odot$ yr^{-1}) $= 5.5 \times 10^{-42} L_{\rm H\alpha}^{\rm SF}$ (erg s^{-1}).

We obtain SFR($L_{\rm H\alpha}^{\rm SF}$) $= [0.03, 19]$ $M_\odot$ yr^{-1}. The median SFR of the AGN in our sample, excluding upper and lower limits, is 7 ± 7 $M_\odot$ yr^{-1}. Those SFRs are among the lowest reported in the literature for samples of non-active star-forming galaxies at similar redshifts and stellar masses, as shown in Table 1.

Thus, by comparing our results with those published in the literature for non-active star-forming galaxies of similar stellar masses and redshifts, we find that our SFRs are lower. Despite the small size of the samples involved in this comparison, this could imply that either

Table 1: Comparison with SFRs (from Hα) of non-active star-forming galaxies from the literature. Columns 2 and 3 list the average/median redshift and an estimation of the stellar mass of the samples considered. In the case of our AGN sample, we considered a stellar mass of $\sim 10^{11}$ $M_\odot$, typical of AGN at this redshift [1]. Columns 4, 5, and 6 give the intervals, average, and median SFRs of the different samples, once converted to the [11] IMF.

Work	Redshift	$M_*(M_\odot)$	SFRs	Average SFR	Median SFR
[8]	∼0.8	...	[4, 11]	7	6 ± 3
Rodríguez-Eugenio et al.	∼1	$10^{10.8}$	[5, 64]	23	19 ± 17
[19]	∼1	$> 10^{10.5}$	[4, 90]	66	54 ± 83
[20]	∼0.8	10^{10}	[3, 31]	...	12^{+21}_{-7}
This work	∼0.8	$\sim 10^{11}$	[0.03, 19]	7	7 ± 7

the presence of an AGN in a galaxy at $z \sim 0.8$ may quench its star formation, or we might be seeing a delay between the offset of the star formation and the AGN activity, as observed in the local universe [6, 22].

Acknowledgments

Based on observations made with the William Herschel Telescope operated on the island of La Palma by the Isaac Newton Group in the Spanish Observatorio del Roque de los Muchachos of the Instituto de Astrofísica de Canarias under the CAT programs 18-WHT7/07B, 16-WHT7/08A, 26-WHT11/08B, and 75-WHT23/09A.

References

[1] Alonso-Herrero, A., Pérez-González, P. G., Rieke, G. H., et al. 2008, ApJ, 677, 127

[2] Barmby, P., Alonso-Herrero, A., Donley, J. L., et al. 2006, ApJ, 642, 126

[3] Brusa, M., Fiore, F., Santini, P., et al. 2009, A&A, 507, 1277

[4] Bundy, K., Georgakakis, A., Nandra, K., et al. 2008, ApJ, 681, 931

[5] Cardelli, J. A., Clayton, G. C., & Mathis, J. S. 1989, ApJ, 345, 245

[6] Davies, R. I., Müller Sánchez, F., Genzel, R., et al. 2007, ApJ, 671, 1388

[7] Davis, M., Faber, S. M., Newman, J., et al. 2003, Proc. SPIE, 4834, 161

[8] Doherty, M., Bunker, A., Sharp, R., et al. 2004, MNRAS, 354, L7

[9] Ho, L. C. 2005, ApJ, 629, 680

[10] Kennicutt, R. C. 1998, ARA&A, 36, 189

[11] Kroupa, P. & Weidner, C. 2003, ApJ, 598, 1076

[12] Lutz, D., Mainieri, V., Rafferty, D., et al. 2010, ApJ, 712, 1287

[13] Nandra, K., Laird, E. S., Adelberger, K., et al. 2005, MNRAS, 356, 568

[14] Ramos Almeida, C., Rodríguez Espinosa, J. M., Barro, G., Gallego, J., & Pérez-González, P. G. 2009, AJ, 137, 179

[15] Ramos Almeida, C., Rodríguez Espinosa, J. M., Acosta-Pulido, J. A., et al. 2012, MNRAS, submitted

[16] Ranalli, P., Comastri, A., Zamorani, G., et al. 2012, A&A, 542, 16

[17] Rieke, G. H., Alonso-Herrero, A., Weiner, B. J., et al. 2009, ApJ, 692, 556

[18] Santini, P., Rosario, D. J., Shao, L., et al. 2012, A&A, 540, 109

[19] Twite, J. W., Conselice, C. J., Buitrago, F., et al. 2012, MNRAS, 420, 1061

[20] Villar, V., Gallego, J., Pérez-González, P. G., et al. 2011, ApJ, 740, 47

[21] Waskett, T. J., Eales, S. A., Gear, W. K., et al. 2004, MNRAS, 350, 785

[22] Wild, V., Heckman, T., & Charlot, S. 2010, MNRAS, 405, 933